Forecasting Pressure Drop and Maximum Sustained Wind Speed Associated with Cyclonic Systems Over Bay of Bengal with Neuro – Computing

Ishita Sarkar
Sutapa Chaudhuri
https://orcid.org/0000-0003-3510-585X
Jayanti Pal (**jayanti.pal@curaj.ac.in**)
Central University of Rajasthan https://orcid.org/0000-0002-0651-6943

Research Article

Keywords: Vortical convective systems, correlation, Multi-layer Perceptron model, forecast, pressure drop, wind speed.

Posted Date: February 17th, 2022

DOI: https://doi.org/10.21203/rs.3.rs-1224432/v1

Abstract

The present research intends to develop a neuro-computing based adaptive intelligent model to predict the pressure drop (PD) at centre and maximum sustained wind speed (MSWS) linked to vortical convective system at the stage of the utmost strength over the Bay of Bengal (BOB) of the North Indian Ocean (NIO). The vortical convective systems considered in this study incorporate the stages from deep depression to extreme severe cyclones. The low level vorticity (LLV), mid-tropospheric relative humidity (MRH), upward wind speed at 850, 500 and 200 hPa pressure levels are obtained as the most suitable input parameters through factor analysis. The adaptive neural network models are trained with the data from 1990 to 2015 to forecast the PD and MSWS over BOB. The result reveals that the multilayer perceptron (MLP) model provides good accuracy at 6 and 30 h lead time in forecasting the PD. But minimum error is obtained at 6 h time before in anticipating the PD at the highest intensity stage of vortical convective system. The result further shows that the MLP model is the most competent for projecting MSWS at the peak intensity stage of vortical convective systems with minimum forecast error at 60 h lead time. The model outputs are compared to the existing conventional models and subsequently the outcomes are supported with observations from 2016 to 2019.

1. Introduction

Tropical cyclones (TCs), vortical convective systems, represent a strong and severe catastrophic warm core low that develop over the tropical ocean bodies. TCs are characterized by strong winds and spiral arrangements of organized thunderstorms that produce heavy rain. Historical records claim that 8 out of 10 cyclonic cases over the North Indian Ocean (NIO) have caused intensive damage in terms of life loss (WMO 2010). From literature (Singh and Singh 2007; Balaguru et al. 2014; Kotal et al. 2019; Wahiduzzaman and Yeasmin 2019), it is evident that the NIO experiences 7% of the world's tropical cyclones. In India, most of TCs strike at east coast causing huge damages (Mohanty et al. 2020). Timely mitigation thus, requires for early prediction of those systems. Prediction of TC has been provided mostly in terms of Intensity and Track. Both these forecasting components depend on pressure drop and wind speed of TCs. During the development of a cyclonic system, the genesis process is controlled by a sequence of events that lead to the development of a self-sustaining warm-cored vortex, which can continue to intensify exclusively due to its own internal dynamics (Alpert et al. 1996; Montgomery et al. 2006; Tory et al. 2006) once formed. The vortical convective systems become extremely non-linear in its developing or weakening stages and, the predictions of the systems are often associated with huge error (Osuri et al. 2012, 2013).

Since the last two decades, several operational and research communities are associated with improvements in the forecast proficiency using various statistical as well as dynamical modelling approaches. Osuri et al. (2012, 2013) used the Weather Research and Forecasting (WRF) model for TC track and intensity forecasts in near real-time across the NIO basin and observes that mean preliminary location and preliminary strength errors are about 57 km and 8–10 m/s respectively. The forecast inaccuracies during the simulation of the severe cyclone JAL and the very severe cyclone THANE have

been appreciably reduced due to the improved observations and assimilation methods which are efficiently integrated in Advanced Research WRF (ARW). (Yesubabu et al. 2014). The study by Osuri et al. (2017) showed an improvement to predict the speedy intensification of TC PHAILIN using advanced HWRF model. India Meteorological Department (IMD) used several models based on statistics and dynamics, employed from numerous domestic and worldwide associations (Mohapatra et al. 2013a; Mohapatra and Sharma 2019) along with one-model ensemble prediction system (EPS) which is part of various global as well as multi-model ensembles (MME) to provide good quality possible forecast of TC over the NIO (Kotal and Roy Bhowmik 2011; Mohapatra et al. 2013b). As per the report of IMD, a recent prediction of very severe cyclone “BULBUL” were quite good but it poses error (RMSE) of about 9.2, 9.2 and 11.3 knots for forecasting hour of 24, 48 and 72 respectively.

Several studies over the NIO (Mohanty et al. 2015; Osuri et al. 2017; Bhala chandran et al. 2019; Kotal et al. 2019; Nadimpalli et al. 2019) have make use of dynamical models to foretell the cyclonic activity in advance. Unlike dynamical model, statistical models mostly have used the statistical information of present and historical TC position for training and thereafter predict position for future time and examine the TC behaviour. Several models have been built for probabilistic TC prognostication, together with the HURRAN-Hurricane.; multiple regression model-CLIPER (Climatology-Persistence) which is created using a set of polynomial regression using several predictors (Vickery et al. 2000); Markov Chain Monte Carlo simulation (Emanuel et al. 2006), and so on. Even though many models from statistics background, are accessible for foreseeing the intensity of vortical convective systems over the Atlantic, eastern north Pacific and western north Pacific basins (DeMaria and Kaplan 1994, 1999; Law and Hobgood 2007), however, the studies over the NIO are limited.

The development of cutting-edge technique like artificial intelligence and related adaptive artificial neural network (ANN) models have emerged as new alterative for the oceanic, and atmospheric studies (Hsieh and Tang 1998; Ali et al. 2007; Chaudhuri et al. 2011, 2013). ANN technique was effective in several remote sensing application areas, such as cloud detection, cloud motion detection, road network detection (Brad and Letia 2002; Barsi and Heipke 2003; Jang et al. 2006) as well as in different applications in meteorology including temperature nowcasting (Lanza and Cosme 2002); long-rang flood forecasting (Jin et al. 1999); typhoon track prophecy (Yang and Wang 2005) etc. Baik and Paek (2000) found that model based on the neural network technique performed better than the multiple linear regression techniques to predict tropical cyclone intensity changes in the western North Pacific up to 72 hours. Lee (2009) projected typhoon storm surge in Taiwan using the back propagation neural network (BPNN) model. Artificial intelligence technique has been successfully used in cyclogenesis prediction over the NIO (Chaudhuri et al. 2014), maximum wind speed prediction of TCs over NIO (Chaudhuri et al. 2017), forecasting severe thunderstorm over Kolkata (Chaudhuri 2010) and so many.

The present study is intended to predict the maximum PD and MSWS of vortical convective systems over BOB. This will aid in predicting the type of TC with adequate lead time. It is evident that both intensity and track are very essential component for forecasting cyclogenesis, however, the present study is concerned on the category prediction of a cyclonic system, considering maximum intensity as target output. Most of

the cited studies have predicted maximum wind speed to predict intensity. Fifty-seven vortical convective systems that take place from 1990 to 2019 over the BOB have been counted in current study. The study has utilised different neural network models, considering essential parameters and their association with PD and MSWS. Particulars of the materials used in present study have been contended in section 2 along with the methodology implemented and execution procedure. In section 3, outcomes of the present study have been argued in detail followed by conclusion in section 4.

2. Data And Methodology

2.1 Data

The dataset considered in this study comprises the records of vortical convective systems reported over the BOB and collected from IMD Best Track during the period from 1990 to 2019 (http://www.rsmcnewdelhi.imd.gov.in). The best track data is available in the Annual Cyclone Review reports and Annual Regional Specialized Meteorological Centre (RSMC) reports published by IMD. The selection is based on best data available and provided by IMD. The variables considered are sea surface temperature (SST), mid-tropospheric relative humidity (MRH), equivalent potential temperature difference (EPTD), inverse of wind shear (IWS), low level vorticity (LLV) at 10 m above sea level and the upward wind velocity (omega) at 850, 500 and 200 hPa pressure levels. The parameters SST, MRH, EPTD, IWS, & LLV are referred to as the central genesis parameters for cyclogenesis (Gray 1975). The daily SST data has been taken from the National Oceanic and Atmospheric Administration (NOAA) (Reynolds et al. 2007) Optimum Interpolation ST V2 which provides data at spatial resolution of 0.25° x 0.25°. The information of upward wind velocity at different pressure levels along with other parameters (temperature, specific humidity, relative humidity, and wind) have been used from National Centres for Environmental Prediction–National Centre for Atmospheric Research (NCEP-NCAR) reanalysis (Kalnay et al. 1996) at 2.5° x 2.5° resolutions. As the study concerns about the intensification of cyclonic system, vertical velocity has been taken as proxy of synoptic-scale precursors to TC rapid intensification (Grimes and Mercer 2015). The MRH is the mean of the relative humidity from 500 hPa to 600 hPa pressure levels. The EPTD has been determined using the temperature and specific humidity data in the middle of surface and 500 hPa levels. The IWS estimated as difference of wind speed between 850 hPa and 200 hPa pressure level wind data. The LLV at 10m has been computed from the Cross-Calibrated Multi-Platform (CCMP) Ocean Surface Wind Vector (Atlas et al. 2011). CCMP delivers a steady, gap-free long-term ocean surface wind vector fields at 10m above sea level from 10th July, 1987 to 30th May 2016 at 0.25° x 0.25° spatial resolutions and 6-hour temporal resolutions. Low level relative vorticity is one of the prime factors for formation of tropical cyclone as it indicates pre-existing disturbances (Singh et al. 2016). The values of all meteorological parameters at the centre of the storm have been calculated by averaging four nearest grid data of original lat/long of TCs. Latitude, Longitude has been taken from IMD best track data. The quantities of PD and MSWS at the following stages of vortical convective systems are also collected from IMD best track data. The dataset used in this study has been break up into two parts: (a) the data from 1990 to 2015 used to train and evaluate the models and (b) the data from 2016

to 2019 has been utilised to validate best model. For validation LLV at 10m has been computed from the SCATSAT-1 Level 4 (operational version 1.0) gridded wind vector data obtained at 10 m above sea level at 25 km spatial resolution. SCATSAT-1 data are available through the SAC-ISRO website (www.mosdac.gov.in). Cyclone KYANT, NADA, MAARUTHA; Severe Cyclone MORA, PHETHAI; Vere Severe Cyclone VARDAH, TITLI, GAJA, BULBUL; and Extreme Severe Cyclone FANI have been considered for validation. In this present study, no Super cyclone has been considered due to limitation of sample.

2.2 Methodology

The statistical method and the artificial intelligence technique have been implemented in this study as the methodologies. Statistical method has been adopted to evaluate the data and ANN has been used to build the forecast models. The Box-Whisker plots (Chaudhuri and Middey 2011) is used to acquire the inconsistency in the parameters associated with the vortical convective systems using low, first quartile, median, third quartile and high. The method of factor analysis has been implemented to pre–sort the data field to line up the ANN models. Factor analysis can be largely categorized as a set of multivariate statistical methods for data lessening and to recognise the final variables by controlling the number and kind of common factors (Fabrigar et al. 1999). Factor analysis requires to keep factors until additional factors account for trivial variance; however, distinct methods of identifying the number of factors to retain often results in different solutions. One of the most used methods is the Kaiser criteria, which retains factors with eigenvalues greater than 1 (Kaiser 1960).

In the present study, ANN model of different category like multi-layer perceptron (MLP), radial basis function networks (RBFN), generalized regression neural network (GRNN) are endeavoured with designated parameters as inputs to recognise the finest network to guess the precise class of the cyclonic system over BOB by estimating the respective PD and MSWS at maximum intensity. The multi-layer perceptron (MLP) is perhaps the most popular ANN architecture in use (Chaudhuri 2010) that employs feed-forward network, typically skilled with back propagation (BP) algorithm. The BP algorithm functions by iteratively altering the connecting weightage of the network to lessen the model inaccuracy. Mathematically this can be expressed as;

$$y = \varphi\left(\sum_{i=1}^{n} \omega_i x_i + b\right) = \varphi\left(w^T x + b\right) \qquad (1)$$

where, w is the vector of weights, x signifies the vector of inputs, b is representing the bias of model and ϕ is the activation function. The radial basis function network (RBFN), a unique ANN employing radial basis function as its triggering function has applied for function guesstimate, curve matching, time series extrapolation, and control and classification problems (Park and Sandberg 1991). In the present study, a Gaussian activation function is used for RBFN;

$$\Phi_j(X) = \left| -(X-\mu_j)^T \sum_j (X-\mu_j)^{-1} \right| \qquad (2)$$

For j = 1...L where L defines the number of concealed unit and X in the input data matrix. μ_j and Σare the mean and covariance matrix of the j^{th} Gaussian function. A simplified regression neural network (GRNN)

is often employed for function approximation. The realization of the GRNN method strongly rely on the distributed factors. The values of distributed factors lie between 0 and 1 were paid to achieve the lowest mean-square error (MSE) for the testing period. Pre-processing of input data has been executed using following calculation (Comrie 1997):

$$O_i^{scaled} = 0.1 + (0.9 \times \frac{O_i - O_{min}}{O_{max} - O_{min}}) \quad (3)$$

Where, O_i, O_{max} and O_{min} are the actual, the highest and the lowest values of variable, respectively.

2.3 Implementation procedure

To develop the ANN models to project the precise class of vortical convective systems, the data and total record of 57 vortical convective systems across BOB have been evaluated during the period from 1990 to 2019. The fifty-seven vortical convective systems over BOB include seven deep depression (DD), eighteen cyclonic storm (CS), nine severe cyclonic storm (SCS), twelve very severe cyclonic storm (VSCS) and eleven extreme severe cyclonic storms (ESCS). The system categorization has been accomplished following the IMD classification (Table 1). In this study, “0” hour for each cyclone has been considered when it was first declared by IMD as “DD” for DD system, “CS” for CS system, “SCS” for SCS system, “VSCS” for VSCS system and “ESCS” for ESCS system (from Best Track data). For example, consider a “SCS” system which has gone through stages DD, CS, SCS while intensifying and while decaying the sequence stages are SCS, CS, DD. Hence “0” hour of this system is the time whenever it attains SCS strength while intensifying. For each system, a single time has been designated as “0” hour. Hence for 57 vortical convective systems there exists 57 “0” hour in target for analysis. Among these 57 vortical convective systems, 47 vortical convective systems have been used to train the ANN model and remaining 10 have been used for validation. The values of the input parameters have been processed from 90 to 6 hour before reaching the greatest intensity (“0” hour) with 6-hour interval for each cyclonic system. The PD and MSWS at “0” hour of each systems has been counted as the target output.

Table 1

The detailed classification of the low-pressure systems and associated pressure drop, maximum sustained wind speed (MSWS) and T number for North Indian Ocean provided by Indian Meteorological Department

(source: http://www.rsmcnewdelhi.imd.gov.in/images/pdf/cyclone-awareness/terminology/faq.pdf*)*

Vortical convective systems	Pressure deficient (hPa) w.r.t T. No.	Wind criteria (Knots)	T-No
Low	1.0	<17	T 1.0
Depression	1.0-3.0	17-27	T 1.5
Deep Depression	3.0-4.5	28-33	T 2.0
Cyclonic Storm	6.1-10.0	34-47	T 2.5-3.0
Severe Cyclonic Storm	15.0	48-63	T3.5
Very Severe Cyclonic Storm	20.9-29.4	64-89	T 4.0-4.5
Extremely Severe Cyclonic Storm	40.2-65.6	90-119	T5.0-6.0
Super Cyclonic Storm	≥ 80.0	≥ 120	T6.5-8.0

Factor analysis is implemented on “0” hour data that comprises eight parameters to find out the significant parameters. Two factors have been considered having eigenvalue greater than 1. Higher variance has been depicted by factor 1 (F1) (Fig. 1a). Factor loading for eight parameters shows that MRH, vertical speed at 850, 500, and 200 hPa levels have factor loading larger than 0.7 from first factor (F1) while LLV shows factor loading larger than 0.7 from second factor (F2) (Fig. 1b). Hence MRH, LLV, omega 850, omega 500 and omega 200 have been chosen as input parameters to structure the input matrix of the ANN model at each lead time in projecting PD and MSWS of vortical convective systems at “0” hour over BOB during the study period. The inconsistency in each input parameter at different stages of vortical convective systems has been assessed through the Box-Whisker plots. MRH at 500-600 hPa specifies the presence of humid mid layers and is beneficial for intense convection, which performs as the primary process for cyclonic circulation. Upward wind velocity (omega) illustrates updraft and downdraft flow of vortical convective systems. Negative omega portrays updraft and positive signifies downdraft. High value of omega increases the updraft of the TCs. The predictors chosen for the study might not be able to predict the intensity of TCs independently but are useful while perform in mixture. The forecast verification is carried out using neural network models with different architecture with 6-90 h lead time and is validated with observation. To measure the correctness in the prognostication, the mean absolute error (MAE), root mean square error (RMSE), and the prediction error (PE) have been examined using the following formulae;

$$MAE = 1/n \sum_{i=1}^{n} |y_{dp} - y_{da}| \quad (4)$$

$$RMSE = \sqrt{1/n \sum_{i=1}^{n} (y_{da} - y_{dp})^2} \quad (5)$$

$$PE = \frac{\langle |y_{dp} - y_{da}| \rangle}{\langle y_{da} \rangle} \quad (6)$$

Where, □ □ suggests the mean of the complete test set. n represents the number of samples. The model output and real values of the parameters are denoted by Y_{dP} and Y_{dA}, respectively.

3. Results And Discussion

The ANN model has been established to predict the class of vortical convective systems by predicting the PD at the centre of the system and MSWS associated with the system at “0” hour over BOB. The LLV, MRH, vertical velocity at 850 hPa, 500 hPa and 200 hPa have been selected as the input parameters to form the ANN model. The inconsistency in different input and output parameters is estimated through box-whisker plots for different categories of TCs (Figs. 2-7). The inconsistency of “0” hour PD during different category of TCs shows that the inconsistency increases as the severity of the system increases. Maximum inconsistency in PD is observed for the ESCS category of the cyclonic system (Fig. 2a). The inconsistency of “0” hour MSWS during different vortical convective systems depicts the spread of data for each cyclonic category (Fig. 2b). It shows that median of MSWS for DD have value of 30 knots and inconsistency is minimum as attributed from box height. In case of CS, median lies at 40 knots with data varying within 35 to 45 knots; for SCS stage, median lies at 55 knots having maximum inconsistency between 55 and 60 knots at “0” hour. Likewise, MSWS for VSCS category mostly vary between 65 and 75 knots with median at 70 knot. In ESCS category, “0” hour MSWS is found to vary between 90 and 105 knots with median at 101 knot (Fig. 2b). The inconsistency in different input parameters has been estimated during different lead time (6-90 h) for each class of TCs. Fig. 3 shows the inconsistency in MRH during different lead time hours for each class of TC. The minimum inconsistency in MRH is observed at 18, 24, 60, 30 and 42 h lead times for DD, CS, SCS, VSCS and ESCS categories of TCs respectively (Fig. 3a-e). The results further show that the inconsistency in MRH increases with lead time for CS, VSCS and ESCS categories of TCs. However, the inconsistency in MRH fluctuates with lead time for DD and SCS categories. The inconsistency in LLV during different lead time from 6 to 90 h for each category of TCs has been estimated (Fig. 4). LLV has minimum inconsistency at 78 hours before “0” hour for DD and SCS while for CS and VSCS, least inconsistency has been observed at 90 hours before “0” hour. For ESCS, minimum inconsistency of LLV has observed at 54 hours before “0” hour (Fig. 4a - e). The results show that the value of LLV is less during minimum inconsistency for all the categories of TCs. The results further show that the inconsistency in LLV decreases with increase in lead time for the DD, CS, and SCS categories of TCs. The inconsistency in LLV fluctuates with lead time for VSCS category. However, the inconsistency in LLV first decreases and then increases with lead time for ESCS stage.

The inconsistency in upward wind velocity at low level (850 hPa) has been evaluated during different categories of TCs (Fig. 5). The minimum inconsistency in omega (850 hPa) is observed at 78, 90, 60, 6 and 36 h lead times for DD, CS SCS, VSCS and ESCS categories of TCs respectively (Fig. 5a-e). The results show that the value of omega is positive / negative during minimum inconsistency for DD, CS, SCS / VSCS, ESCS categories of TCs. The results further show that the inconsistency in omega (850 hPa) increases with lead time for VSCS category whereas the inconsistency in omega (850 hPa) fluctuates with lead time hour for DD, CS, SCS and ESCS categories of TCs. The inconsistency in vertical velocity at mid-level (500 hPa) has been estimated for different stages of TCs (Fig. 6). Omega (500 hPa) has minimum inconsistency at 66 hours before “0” hour for DD; while for CS and SCS, least inconsistency has been observed at 84 hours before “0” hour. For VSCS, minimum inconsistency has been observed at 18 hours before “0” hour and for ESCS, minimum inconsistency of Omega (500 hPa) has been observed at 90 hours before “0” hour (Fig. 6a-e). The results show that the value of vertical velocity at mid-level (500 hPa) is positive / negative during minimum inconsistency for DD / CS, SCS, VSCS, and ESCS categories of TCs. The results further show that the inconsistency in vertical velocity at mid-level (500 hPa) increases with lead time for the VSCS category, whereas the inconsistency decreases with lead time for the DD, CS and SCS categories of TCs. However, the inconsistency in the vertical velocity at 500 hPa fluctuates with lead time for ESCS category. The inconsistency in vertical velocity at 200 hPa level has been estimated for different stages of TCs (Fig. 7). The minimum inconsistency in vertical velocity at 200 hPa is observed at 72, 90, 60, 84 and 90 h lead times for DD, CS, SCS, VSCS and ESCS categories of TCs respectively (Fig. 7a - e). The results show that the value of vertical velocity at 200 hPa is positive / negative during minimum inconsistency for SCS / DD, CS, VSCS, and ESCS categories. The results further show that the inconsistency in vertical velocity at 200 hPa increases with lead time for VSCS category, whereas the inconsistency decreases with lead time for the DD, CS and SCS categories. However, the inconsistency in the vertical velocity at 200 hPa fluctuates with lead time for ESCS category. The neural nets are constructed with different architectures to select the best one for forecasting the PD and MSWS of TCs over BOB up to 90h lead time with the input parameters of MRH, LLV, vertical velocity at 850 hPa, 500 hPa and 200 hPa collected at 90 to 6 h before attaining the highest intensity. A comparative study with multi-layer perceptron (MLP), radial basis function network (RBFN), and generalized regression neural network (GRNN) models are made for the purpose. Ten different neural nets with maximum 3 hidden layers and up to 5 nodes at each hidden layer have been trained with back-propagation training algorithm with 90 h lead time to identify the best for forecasting PD and MSWS of TCs over BOB at “0” hour. The result shows that the minimum train error is obtained from the MLP model at each forecast hour for PD and MSWS forecast. Fig. 8a shows the train error of ten neural network models obtained at each forecast hour in forecasting the central PD. The detailed configuration of 15 best MLP models, with minimum train error, obtained from each forecast hour in forecasting PD is described (Table 2). The prediction error (PE), mean absolute error (MAE), and root mean square error (RMSE) have been computed to find out the skill of the models. The minimum prediction error is observed at 6 h lead time in forecasting the PD of the TCs at “0” hour over BOB. The values of MAE and RMSE are also found minimum at 6 h lead time (Fig. 8b). It is also observed that MAE, PE and RMSE slightly increase at 12 h lead time, subsequently the error decreases till 30 h lead time. The result further shows that the errors are

comparatively higher thereafter. During validation of the model with observation, minimum error has also found at 6 h lead time. Likewise, the train error of 10 different neural network models has been computed to find out the skill of the models in forecasting MSWS of TCs at “0” hour over BOB (Fig. 9a). The evaluation of the error during MSWS forecast also depicts that the minimum train error is obtained through the MLP models at each forecast hour. The configuration of 15 best MLP models with minimum error obtained at each lead time is described (Table 3). The minimum prediction error in forecasting the MSWS of TCs at “0” hour is observed with the MLP model at 60 h lead time. Evaluation of MAE and RMSE reveals that error is minimum with MLP model at 60 h lead time (Fig. 9b). During validation of the model product, minimum error has been observed at 60 h lead time (Fig. 9c).

Table 2
The Architecture of the model having minimum train error at each lead time for forecasting pressure drop at 0 hour

Lead Time (Hour)	Model Architecture
6	MLP 5:5-4-4-1:1
12	MLP 5:5-4-1:1
18	MLP 5:5-4-3-1:1
24	MLP 5:5-4-3-1:1
30	MLP 5:5-4-4-1:1
36	MLP 5:5-1-2-1:1
42	MLP 5:5-4-3-1:1
48	MLP 5:5-1-1:1
54	MLP 5:5-5-1:1
60	MLP 5:5-2-1:1
66	MLP 5:5-1-1:1
72	MLP 5:5-1-1:1
78	MLP 5:5-1-1:1
84	MLP 5:5-1-1:1
90	MLP 5:5-2-1:1

Table 3

The Architecture of the model having minimum train error at each lead time for forecasting maximum sustained wind speed (MSWS) at 0 hour

Lead Time (Hour)	Model Architecture
6	MLP 5:5-5-1:1
12	MLP 5:5-4-4-1:1
18	MLP 5:5-5-4-1:1
24	MLP 5:5-3-1:1
30	MLP 5:5-4-3-1:1
36	MLP 5:5-4-1:1
42	MLP 5:5-3-1:1
48	MLP 5:5-4-1:1
54	MLP 5:5-5-5-1:1
60	MLP 5:5-5-1:1
66	MLP 5:5-4-4-1:1
72	MLP 5:5-5-5-1:1
78	MLP 5:5-2-1:1
84	MLP 5:5-4-2-1:1
90	MLP 5:5-4-4-1:1

To check the robustness of the results, best ANN model result in PD and MSWS forecast have been compared with lesser number of samples. Figs. 10 and 11 demonstrate the estimated forecast errors for different number of samples in forecasting PD and MSWS. Fig. 10 depicts that the error decreases with increase in number of training samples except when model is trained with minimum number (17) of data-sample. It is also observed that model performs best with 47 data-samples. In case of MSWS, minimum error is obtained when model is trained with 47 data-samples (Fig. 11). Hence 47 data samples are enough to use for model training in present study.

A comparative analysis between prediction from ANN method and corresponding IMD observation has been done (Fig. 12). Fig. 12a shows the predicted PD values in comparison with IMD observation. The result shows that, in some cases, the present model overestimates the PD while the increasing pattern of PD with severity has been well captured by the model (Fig. 12a). Fig. 12b shows the predicted MSWS values in comparison with IMD observation. Here the predicted MSWS with 60 h lead time is well comparable with the IMD observation (Fig. 12b). Validation also shows similar behaviour as the analysis

(Fig. 13). The model predicted central PD with 6 h lead time are found to be closer to the IMD observed PD for most of the cases during validation (Fig. 13a). It is also observed that the values of MSWS obtained from MLP model at 60 h lead time is well comparable with the actual values during validation (Fig. 13b). Fig. 14 shows the sensitivity analysis on the input variables to look at which input parameter is more sensitive to the neural network used for forecasting the PD and MSWS of tropical cyclones. Sensitivity analysis classify the requirement of variables according to the corrosion in modeling performance that occurs if that variable is no longer available to the model. So, it is the ratio of the error with missing value exchange to the original error. The more susceptible the network is to a particular input, the larger the deterioration can be expected, and therefore the larger the ratio. Result shows that MRH has the highest (2.2) influence on the cyclone wind speed change.

4. Skill Comparison Of The Present Model With The Existing Conventional Models

The skill of the present models is assessed by judging its performance with IMD operational forecast model (Table 4). As per the 'IMD Preliminary Report 2019' of IMD, a recent prediction of extremely severe cyclone "FANI" poses error (RMSE) of about 13.5 knots in intensity (wind) forecast for 60 h lead period. The present study endeavored to forecast the category of a cyclonic system in terms of PD and MSWS at the stage of the highest intensity over the BOB with Multi-Layer Perceptron model. The skill of intensity forecast in terms of maximum sustained surface wind is verified by computing the RMSE. The forecast error obtained for cyclone FANI is 9 knots with 60 h lead time (Table 4). Table 4 also shows the skill comparison between present model and IMD prediction for Cyclone KYANT; Severe Cyclone PHETHAI; Very Severe Cyclone VARDAH, TITLI, GAJA, BULBUL. The result shows that the RMSE was less with MLP model for all vortical convective systems except PHETAI & TITLI.

Table 4
Comparison of the present study with IMD operational model

No.	Name of Vortical convective systems	Intensity forecast error (RMSE) in knots at 60h lead time
1.	CS Kyant	Present Study – 5 knot IMD – 13.5 knot
2.	SCS Phetai	Present Study – 10 knot IMD – 8.3 knot
3.	VSCS Vardah	Present Study – 3 knot IMD – 13.2 knot
4.	VSCS Titli	Present Study – 10 knot IMD – 8.3 knot
5.	VSCS Gaja	Present Study – 7 knot IMD – 13.6 knot
6.	VSCS Bulbul	Present Study – 7 knot IMD – 7.6 knot
7.	VSCS Fani	Present Study – 9 knot IMD – 13.5 knot

5. Conclusion

The endeavor of the present research is to develop a neuro–computing based model to observe the forecast efficiency in predicting the PD and MSWS associated with different categories of TCs over the BOB at the stage of the peak intensity with adequate lead time and precision. From literature it is evident that ANN has been widely used in predicting track and intensity while there is very less study on prediction of intensification using ANN. Present study thus, aims to explore and evaluate the intensification using ANN technique. Present study considers eight parameters, and those parameters are analysed for 6 to 90 h lead time from the target “0” hour. Based on factor analysis significant predictors have been selected as input parameter of the model. These are LLV, MRH, and upward wind velocity at 850, 500 and 200 hPa pressure level. The inconsistency of these input parameters as well as output parameter has been evaluated. Three types of ANN models namely, MLP, RBFN and GRNN have been checked to distinguish the finest model for forecasting PD and MSWS associated with different categories of vortical convective systems over BOB of NIO at the stage of the highest intensity. MLP model is found as the most efficient for forecasting PD (model 1) and MSWS (model 2). The architecture of model 1 is 5:5-4-4-1:1 specifying five inputs with two hidden layers having four hidden nodes in each

layer and one output. The model has the competence to forecast PD of cyclones at their highest intensity with 91% accuracy (6 h lead time). The MLP model (model 2) with configuration 5:5-5-1:1 (five input layers, one hidden layer with five nodes and one output layer) was observed to perform best (minimum forecast error) for forecasting maximum wind speed with 60 h lead time. During validation with SCATSAT-1 data, similar result has been observed. MLP is a statistical model, and it completely depends on data statistics. From gradient wind balance, it is observed that the central pressure deficit in a tropical cyclone depends principally on two velocity scales: the maximum azimuthal-mean azimuthal wind speed and half the product of the Coriolis parameter and a measure of outer storm size (Chavas et al. 2017). Hence to make better prediction for PD, other factors are needed to consider.

Declarations

Acknowledgment The corresponding author acknowledges the Space Application Centre, ISRO, India for providing the opportunity to participate in the SCATSAT 1 Application programme. The authors gratefully acknowledge the anonymous reviewers for constructive comments which helped to improve the clarity of the manuscript.

Funding The authors declare that no funds, grants, or other support were received during the preparation of this manuscript.

Competing Interests The authors have no relevant financial or non-financial interests to disclose.

Author contribution All authors contributed to the study conception and design. Jayanti Pal and Ishita Sarkar performed the analyses and wrote the paper. All authors read and approved the final manuscript.

Data availability The datasets analysed during the current study are available in IMD website (http://www.rsmcnewdelhi.imd.gov.in).

Code availability Not applicable.

Ethics approval Not applicable.

Conflict of interest The authors declare no competing interests

References

1. Ali MM, Jagadeesh PSV, Jain S (2007) Effects of eddies and dynamic topography on the Bay of Bengal cyclone intensity. EOS Trans AGU 88 (8): 93–95.
2. Alpert P, Tsidulko M, Krichak S, Stein U (1996) A multistage evolution of an ALPEX cyclone. Tellus A 48:209-220.
3. Atlas R, Hoffman RN, Ardizzone J, Leidner SM, Jusem JC, Smith DK, Gombos D (2011) A Cross-calibrated, Multiplatform Ocean Surface Wind Velocity Product for Meteorological and

Oceanographic Applications. Bull. Amer. Meteor. Soc. 92:157–174.

4. Baik JJ, Paek JS (2000) A neural network model for predicting typhoon intensity. J Meteorol Soc Jpn Ser. II, 78(6): 857-869.
5. Balaguru K, Taraphdar S, Leung LR, Foltz GR (2014) Increase in the intensity of postmonsoon Bay of Bengal tropical cyclones. Geophys Res Lett 41(10): 3594–3601.
6. Barsi A, Heipke C (2003) Artificial neural networks for the detection of road junctions in aerial images. International Archives of Photogrammetry, Remote Sensing and Spatial Information Sciences 34: 113-118 (Part 3/W8).
7. Bhalachandran S, Nadimpalli R, Osuri KK, Marks Jr F, Gopalakrishnan SG, Subramanian S, Mohanty UC, Niyogi D (2019) On the processes influencing rapid intensity changes of tropical cyclones over the Bay of Bengal. Sci Rep 9 3382.
8. Brad R, Letia IA (2002) Cloud motion detection from infrared satellite images. In: Proc. Second International Conference on Image and Graphics (ICIG 2002), vol. 4875, pp. 408-412.
9. Chaudhuri S (2010) Convective energies in forecasting severe thunderstorms with one hidden layer neural net and variable learning rate back propagation algorithm. Asia-Pac J Atmos Sci 46(2):173–183.
10. Chaudhuri S, Middey A (2011) Adaptive neuro-fuzzy inference system to forecast peak gust speed during thunderstorms. Meteorol Atmos Phys 114:139–149.
11. Chaudhuri S, Das D, Middey A, Goswami S (2011) Forecasting the concentration of atmospheric pollutants: skill assessment of auto regressive and radial basis function network. Int J Environ Prot 1(5): 41–47.
12. Chaudhuri S, Dutta D, Goswami S, Middey A (2013) Intensity forecast of tropical cyclones over North Indian Ocean using multi layer perceptron model: skill and performance verification. Nat Hazards 65**:** 97–113.
13. Chaudhuri S, Goswami S, Middey A (2014) Medium-range forecast of cyclogenesis over North Indian Ocean with multilayer perceptron model using satellite data. Nat Hazards 70: 173–193.
14. Chaudhuri S, Basu D, Das D, Goswami S, Varshney S (2017) Swarm intelligence and neural nets in forecasting the maximum sustained wind speed along the track of tropical cyclones over Bay of Bengal. Nat Hazards 87:1413–1433.
15. Chavas DR, Reed KA, Knaff, JA (2017) Physical understanding of the tropical cyclone wind-pressure relationship. Nat commun 8(1):1-11.
16. Comrie AC (1997) Comparing neural networks and regression models for ozone forecasting. *J AIR WASTE MANAGE* 47:653–663.
17. DeMaria M, Kaplan J (1994) A statistical hurricane intensity prediction scheme (SHIPS) for the Atlantic basin. Weather Forecast 9:209–220.
18. DeMaria M, Kaplan J (1999) An updated statistical hurricane intensity prediction scheme (SHIPS) for the Atlantic and east North Pacific basins. Weather Forecast 14:326–337.

19. Emanuel K, Ravela S, Vivant E, Risi C (2006) A Statistical Deterministic Approach to Hurricane Risk Assessment. Bull Amer Meteor Soc 87:299–314.
20. Fabrigar LR, Wegener DT, MacCallum RC and Strahan EJ (1999) Evaluating the use of exploratory factor analysis in psychological research. Psychol. Methods. 4(3):272-299.
21. Gray WM (1975) Tropical cyclone genesis. Dept. of Atmos. Sci. Paper 234, Colorado State University, Fort Collins, CO, 121 pp
22. Grimes A, Mercer AE (2015) Synoptic-scale precursors to tropical cyclone rapid intensification in the Atlantic Basin. Adv Meteorol 2015.
23. Hsieh WW, Tang B (1998) Applying neural network models to prediction and data analysis meteorology and oceanography. Bull Amer Meteor Soc 79:1855–1870.
24. Jang JD, Viau AA, Anctil F, Bartholomé E (2006) Neural network application for cloud detection in SPOT vegetation images. International Journal of Remote Sensing 27(3-4): 719-736.
25. Jin L, Chen N, Lin ZS (1999) Study and comparison of ensemble forecasting based on artificial neural network (in Chinese). Acta Meteorol. Sin. 57:198–207.
26. Kaiser HF (1960) The Application of Electronic Computers to Factor Analysis. Educ Psychol Meas 20(1):141–151.
27. Kalnay E, Kanamitsu M, Kistler R, Collins W, Deaven D, Gandin L, Iredell M, Saha S, White G, Woollen J, Zhu Y, Chelliah M, Ebisuzaki W, Higgins W, Jaccnowiak J, Mo KC, Ropelewski C, Wang J, Leetmaa A, Reynolds R, Jenne R, Joseph D (1996) The NCEP/NCAR 40 - year reanalysis project. Bull Amer Meteor Soc 77:437 – 471.
28. Kotal SD, Roy Bhowmik SK (2011) A multimodel ensemble (MME) technique for cyclone track prediction over the North Indian Sea. Geofizika 28(2)**:**275-291.
29. Kotal SD, Bhattacharya SK, Roy Bhowmik SK (2019) Estimation of Tropical Cyclone Intensity and location over the North Indian Ocean-a Challenge. Met Application 26(2):245-252.
30. Lanza PA, Cosme JM (2002) A short-term temperature forecaster based on a state space neural network. Eng Appl Artif Intell 15:459–464.
31. Law KT, Hobgood JS (2007) A statistical model to forecast short-term Atlantic hurricane intensity. Weather Forecast 22:967–980.
32. Lee TL (2009) Prediction of typhoon storm surge using artificial neural network. Adv. Eng. Softw 40:1200–1206.
33. Mohanty S, Nadimpalli R, Mohanty UC, Mohapatra M, Sharma A, Das AK, Sil S (2020) Quasi-operational forecast guidance of extremely severe cyclonic storm Fani over the Bay of Bengal using high-resolution mesoscale models. Meteorol Atmos Phys 22:1-8.
34. Mohanty UC, Osuri KK, Tallapragada V, Marks FD, Pattanayak S, Mohapatra M, Gopalakrishnan SG, Niyogi D (2015) A great escape from the Bay of Bengal 'Super Sapphire-Phailin' tropical cyclone—a case of improved weather forecast and societal response for disaster mitigation. Earth Interact 19(17):1–11.

35. Mohapatra M, Nayak DP, Sharma RP, Bandyopadhyay BK (2013b) Evaluation of official tropical cyclone track forecast over north Indian Ocean issued by India Meteorological Department. J Earth Syst Sci 122(3):589-601.
36. Mohapatra M, Sikka DR, Bandyopadhyay BK, Tyagi A (2013a) Outcomes and challenges of Forecast Demonstration Project (FDP) on landfalling cyclones over Bay of Bengal. Mausam 61(1):1-12.
37. Mohapatra M, Sharma M (2019) Cyclone warning services in India during recent years: A review. MAUSAM 70(4):635-666.
38. Montgomery MT, Nicholls ME, Cram TA, Saunders AB (2006) A vortical hot tower route to tropical cyclogenesis, J Atmos Sci 63:355–386.
39. Nadimpalli R, Osuri KK, Mohanty UC, Das AK, Kumar A, Sil1 S, Niyogi D (2019) Forecasting Tropical Cyclones in the Bay of Bengal using quasi-operational WRF and HWRF modeling systems: an assessment study. Meteorol Atmos Phys 132(5):1–17.
40. Osuri KK, Mohanty UC, Routray A, Kulkarni MA, Mohapatra M (2012) Sensitivity of physical parameterization schemes of WRF model for the simulation of Indian seas tropical cyclones. Nat Hazards 63(3):1337–1359.
41. Osuri KK, Mohanty UC, Routray A, Mohapatra M, Niyogi D (2013) Real-time track prediction of tropical cyclones over the North Indian Ocean using the ARW model. J Appl Meteorol Climatol 52(11):2476–2492.
42. Osuri KK, Nadimpalli R, Mohanty UC, Niyogi D (2017) Prediction of rapid intensification of tropical cyclone Phailin over the Bay of Bengal using the HWRF modelling system. Q J R Meteorol Soc 143:678–690.
43. Park J, Sandberg IW (1991) Universal approximation using radial-basis function networks. Neural Comput 3(2):246-257.
44. Reynolds RW, Smith TM, Liu C, Chelton DB, Casey KS, Schlax MG (2007) Daily high-resolution-blended analyses for sea surface temperature. J Clim 20:5473–5496.
45. Singh D, Singh V (2007) Impact of tropical cyclone on total ozone measured by TOMS–EP over the Indian region. Curr Sci 93(4):37–42.
46. Singh K, Panda J, Osuri KK, Vissa NK (2016) Progress in tropical cyclone predictability and present status in the North Indian Ocean region. In recent developments in tropical cyclone dynamics, prediction, and detection. 193-215.
47. Tory KJ, Montgomery MT, Davidson NE (2006) Prediction and diagnosis of tropical cyclone formation in an NWP system. Part I: The critical role of vortex enhancement in deep convection. J Atmos Sci 63:3077–3090.
48. Vickery PJ, Skerjl P, Steckley AC, Twinsdale L (2000) Simulation of hurricane risk in the United States using an empirical storm track modeling technique. J Struct Eng 126:1222–1237.
49. Yesubabu V, Srinivas CV, Hariprasad KBRR, Baskaran R (2014) A study on the impact of observation assimilation on the numerical simulation of tropical cyclones JAL and THANE using 3DVAR. Pure Appl Geophys 171(8):2023–2042.

50. Wahiduzzaman M, Yeasmin A (2019) Statistical forecasting of tropical cyclone landfall activities over the North Indian Ocean rim countries. Atmos Res 227:89-100.
51. World Meteorological Organization Technical Document (2010) Tropical cyclone operational plan for the Bay of Bengal and the Arabian Sea, Document, Edition 2010, WMO/TD 84.
52. Yang YQ, Wang JZ (2005) An integrated decision method for prediction of tropical cyclone movement by using genetic algorithm. Sci. China (D) 48:52–68.

Figures

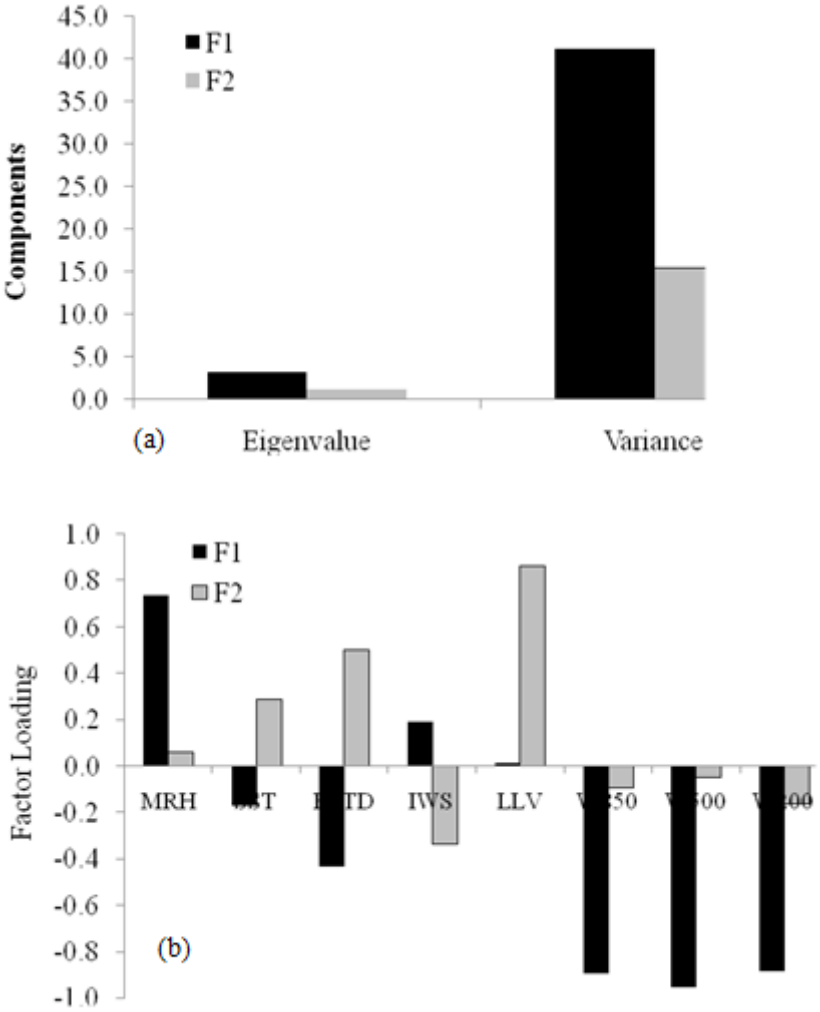

Figure 1

Factor analysis of parameters at “0” hour provided (a) eigen value and variance explained by two principal factors and (b) factor score for selected parameters.

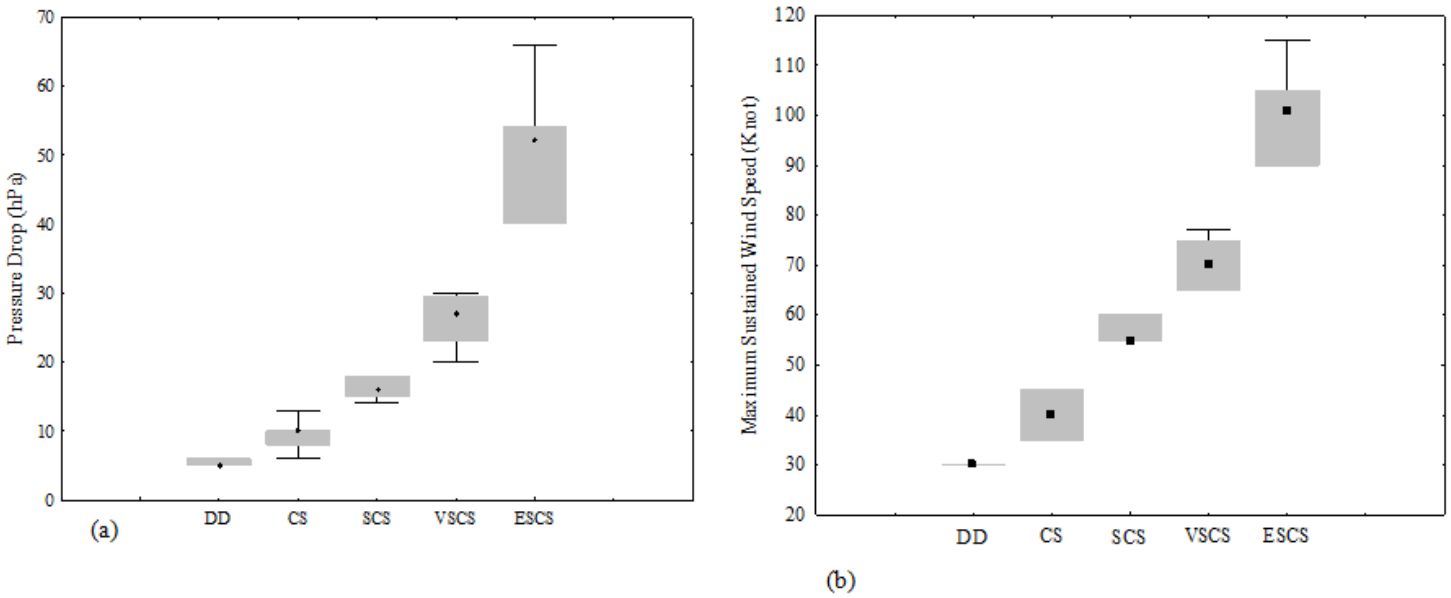

Figure 2

Inconsistency in (a) Pressure drop (hPa) and (b) Maximum sustained wind speed (kts) for Deep Depression (DD), Cyclonic Storm (CS), Severe Cyclonic Storm (SCS), Very Severe Cyclonic Storm (VSCS) and Extreme Severe Cyclonic Storm (ESCS) over Bay of Bengal

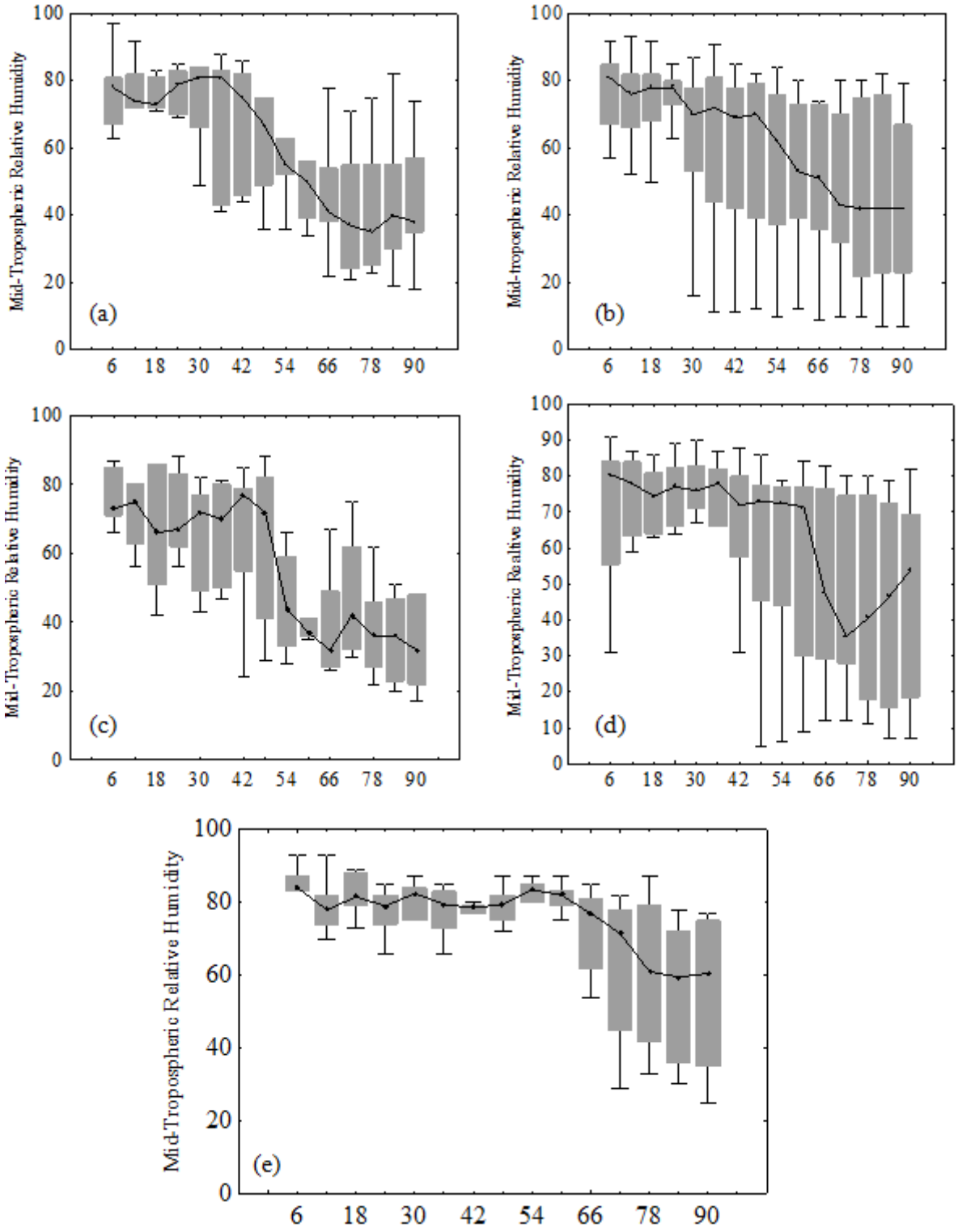

Figure 3

Inconsistency in Mid-Tropospheric Relative humidity (MRH) at lead time 6-90 hour for (a) Deep Depression (DD), (b) Cyclonic Storm (CS), (c) Severe Cyclonic Storm (SCS), (d) Very Severe Cyclonic Storm (VSCS) and (e) Extreme Severe Cyclonic Storm (ESCS) over Bay of Bengal

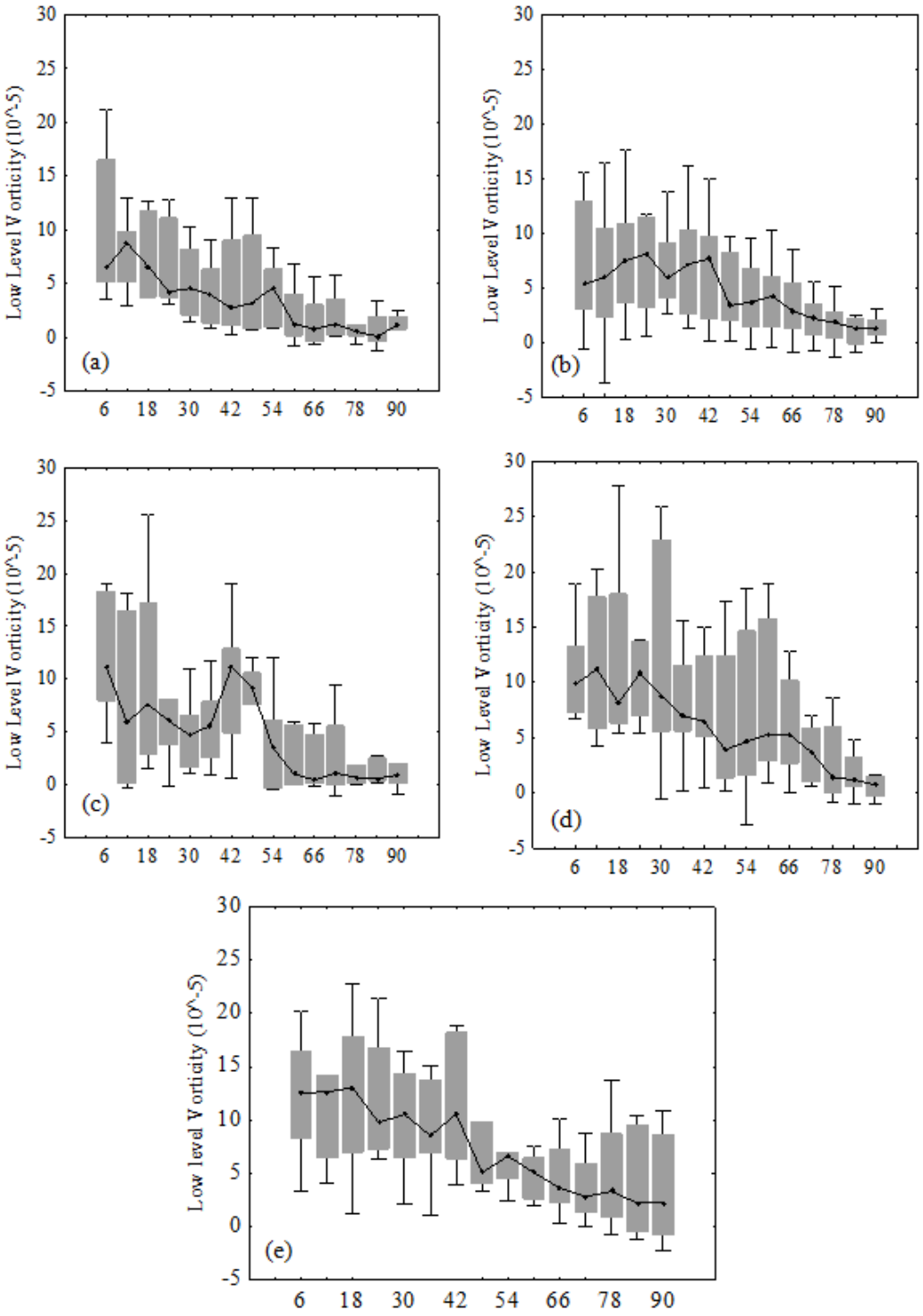

Figure 4

Inconsistency in Low Level Vorticity (S^{-1}) at lead time 6-90 hour for (a) Deep Depression (DD), (b) Cyclonic Storm (CS), (c) Severe Cyclonic Storm (SCS), (d) Very Severe Cyclonic Storm (VSCS) and (e) Extreme Severe Cyclonic Storm (ESCS) over Bay of Bengal.

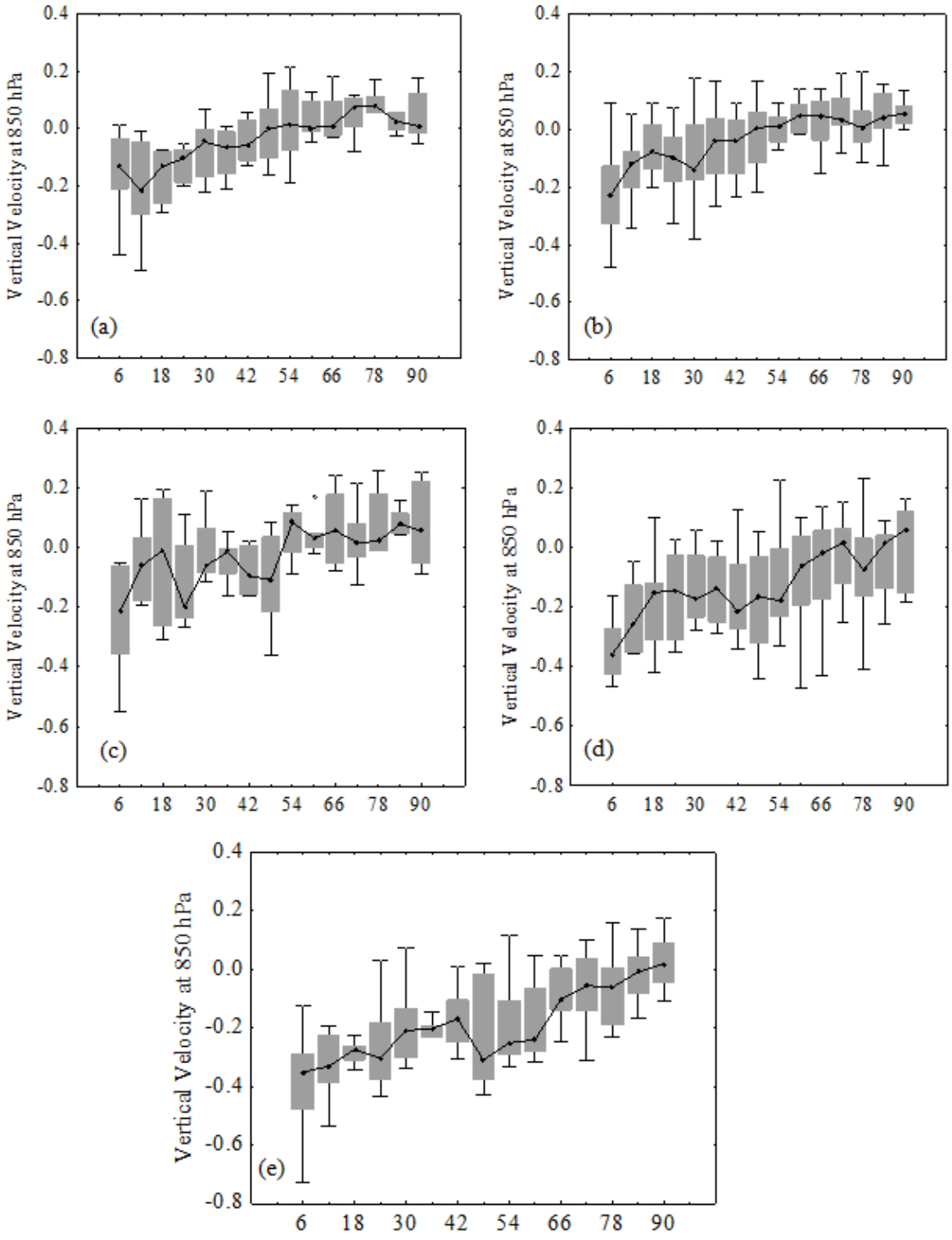

Figure 5

Inconsistency in Vertical Velocity (Pa/s) at 850 hPa at lead time 6-90 hour for (a) Deep Depression (DD), (b) Cyclonic Storm (CS), (c) Severe Cyclonic Storm (SCS), (d) Very Severe Cyclonic Storm (VSCS) and (e) Extreme Severe Cyclonic Storm (ESCS) over Bay of Bengal.

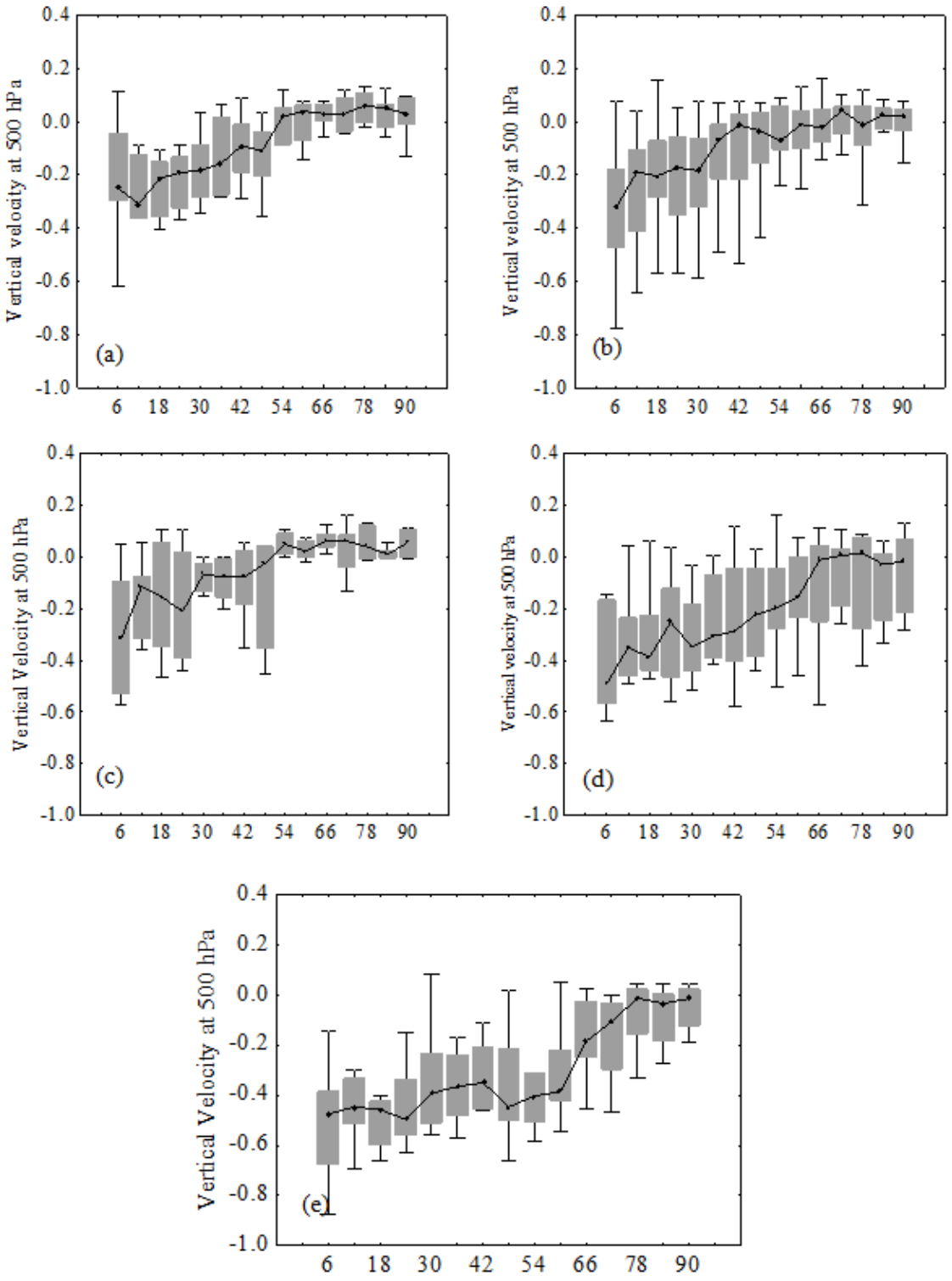

Figure 6

Inconsistency in Vertical Velocity (Pa/s) at 500 hPa at lead time 6-90 hour for (a) Deep Depression (DD), (b) Cyclonic Storm (CS), (c) Severe Cyclonic Storm (SCS), (d) Very Severe Cyclonic Storm (VSCS) and (e) Extreme Severe Cyclonic Storm (ESCS) over Bay of Bengal.

Figure 7

Inconsistency of Vertical Velocity (Pa/s) at 200 hPa at lead time 6-90 hour for (a) Deep Depression (DD), (b) Cyclonic Storm (CS), (c) Severe Cyclonic Storm (SCS), (d) Very Severe Cyclonic Storm (VSCS) and (e) Extreme Severe Cyclonic Storm (ESCS) over Bay of Bengal.

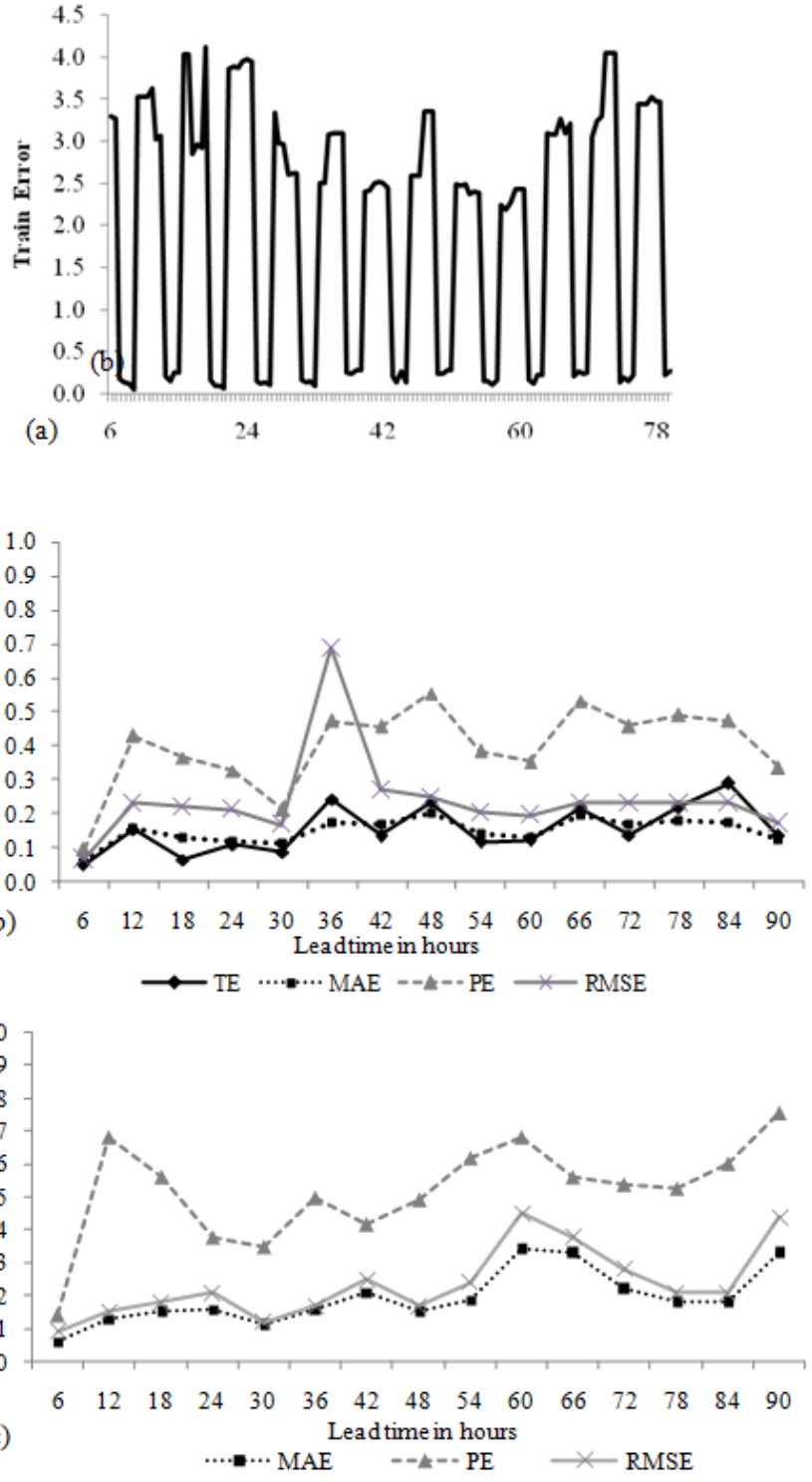

Figure 8

Forecast errors including (a) train error of ten neural network models (b) prediction error, mean absolute error and root mean square error during training period and (c) prediction error, mean absolute error and root mean square during validation in forecasting the central pressure drop using Multi-Layer Perceptron model with 6-90 h lead time

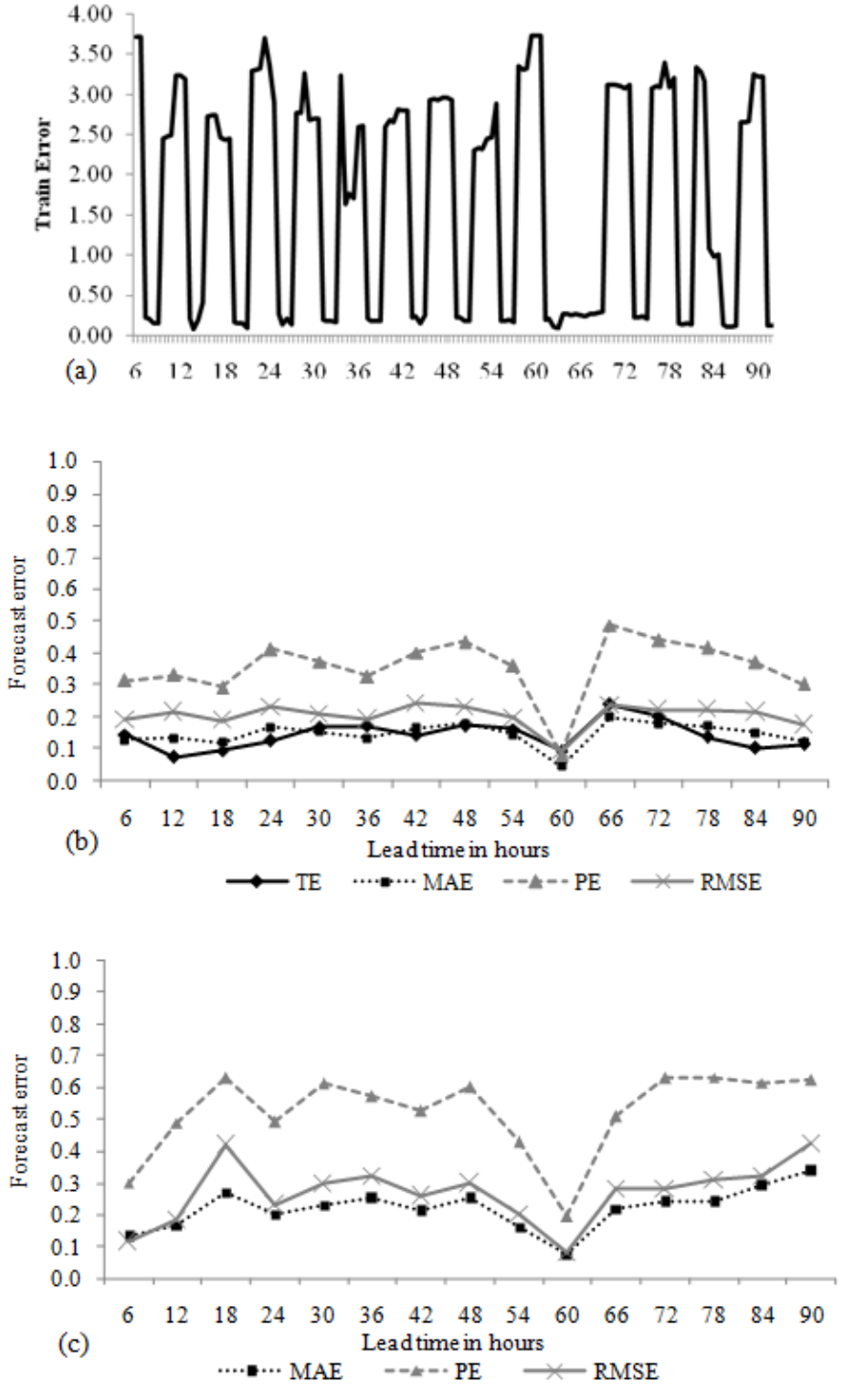

Figure 9

Forecast errors including (a) train error of ten neural network models (b) prediction error, mean absolute error and root mean square error during training period and (c) prediction error, mean absolute error and root mean square during validation in forecasting the maximum sustained wind speed using Multi-Layer Perceptron model with 6-90 h lead time

Figure 10

Forecast error against number of input data-samples in forecasting Pressure Drop (PD) at 6 hour lead time

Figure 11

Forecast error against number of input data-samples in forecasting Maximum sustained wind speed (MSWS) at 60 hour lead time

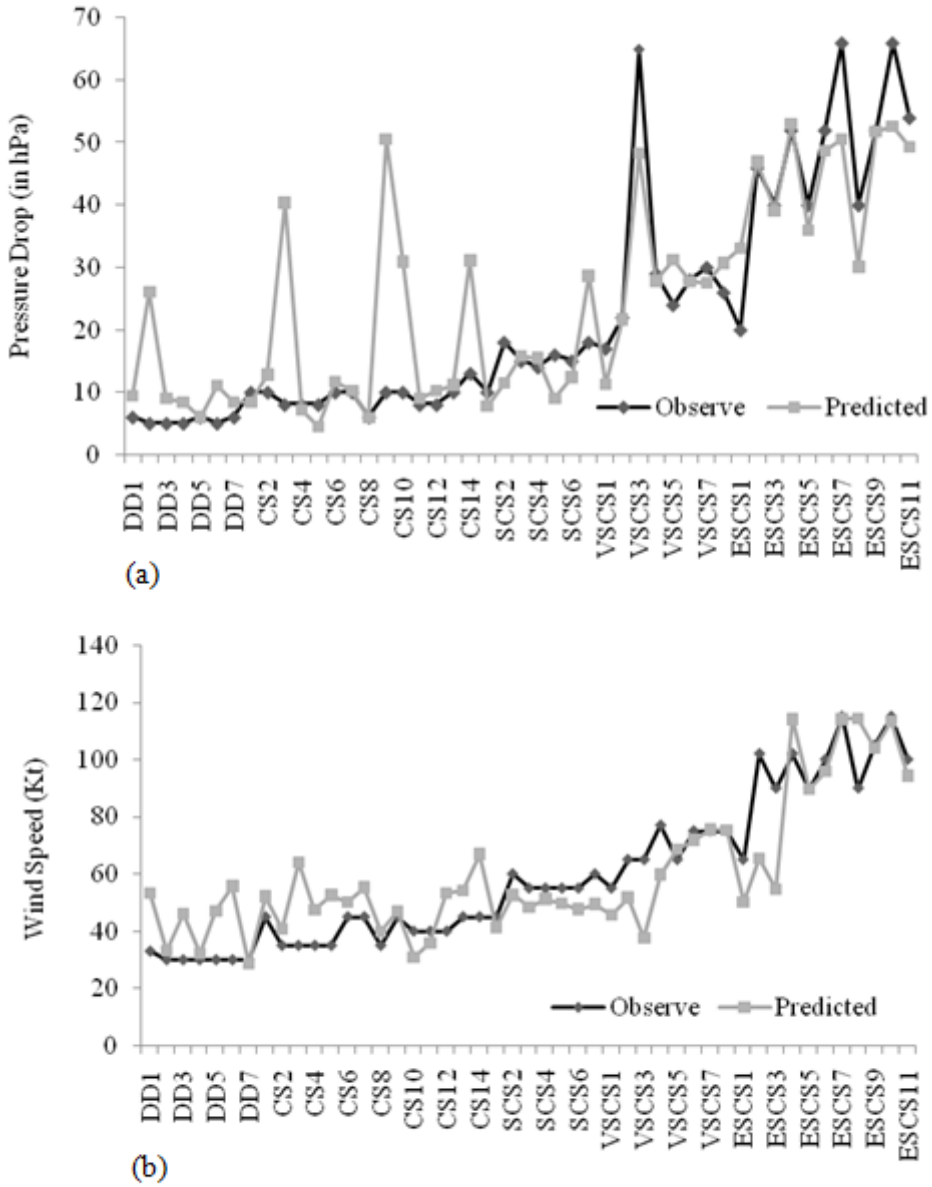

Figure 12

Comparison of Observed and Predicted (a) Pressure drop (PD) at 6 hour lead time and (b) Maximum sustained wind speed (MSWS) at 60 hour lead time during analysis

Figure 13

Comparison of Observed and Predicted (a) Pressure drop (PD) at 6 hour lead time and (b) Maximum sustained wind speed (MSWS) at 60 hour lead time during validation.

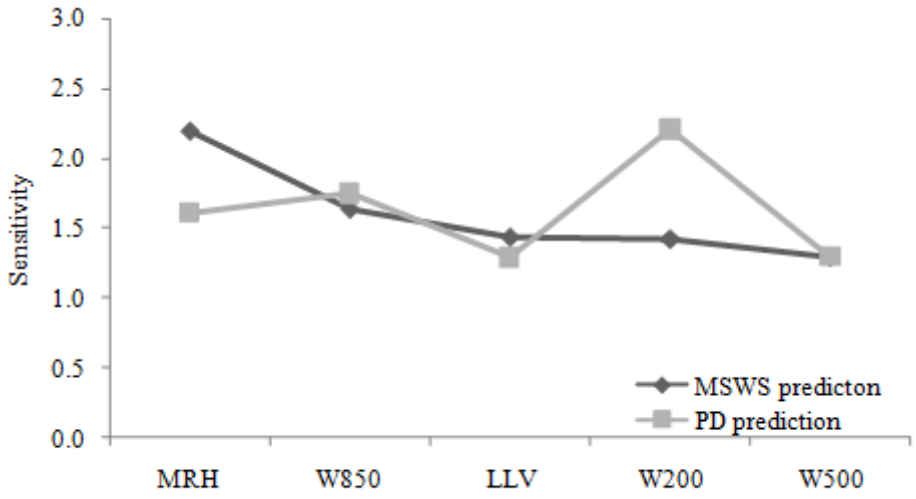

Figure 14

Sensitivity analysis on the input parameters to the neural network model for forecasting Pressure drop and Maximum sustained wind speed of tropical cyclones over BOB